ELSEVIER International Journal of Mass Spectrometry 220 (2002) 211–220
International Journal of Mass Spectrometry
www.elsevier.com/locate/ijms

Electron attachment to C_2F_5I molecules and clusters

Judith Langer, Stefan Matejcik[1], Eugen Illenberger[*]

Institut für Chemie-Physikalische und Theoretische Chemie, Freie Universität Berlin, Takustrasse 3, D-14195 Berlin, Germany

Received 15 October 2001; accepted 24 December 2001

Abstract

Electron attachment reactions to single C_2F_5I molecules and to C_2F_5I clusters are studied in a crossed electron beam/molecular beam experiment with mass spectrometric detection of the ionic products. In single molecules we observe I^- and F^- formed by dissociative electron attachment (DA) with I^- appearing from a narrow resonance near 0 eV and F^- from a broad and structured feature composed of three overlapping resonances in the energy range between 1.5 and 6.5 eV. In electron attachment to clusters the undissociated ions $M_n{}^-$ and solvated fragment ions of the form $I^-{\cdot}M_n$ and $F^-{\cdot}M_n$ ($M = C_2F_5I$) are additionally generated. The solvated fragment $I^-{\cdot}M$ is considerably more abundant than the stabilized monomer anion M^- which is a mirror of the early steps in the evolution of the transient anion in the cluster. The pronounced impulsive dissociation into I^- obviously prevails intracluster decomposition over collisional stabilization (caging effect). The solvated ions $I^-{\cdot}M_n$ appear (in addition to the low energy resonance) via structured contributions at higher energy indicating that they are the result of inelastic electron scattering processes (autoscavenging) in the target cluster. By using the seed gas Ar in large excess (1:100) in the expansion, complexes of the form $Ar_n{\cdot}I^-$, $Ar_n{\cdot}M^-$ and, most remarkably, also the ternary cluster ions $Ar_n{\cdot}M{\cdot}I^-$ are observed. (Int J Mass Spectrom 220 (2002) 211–220)

© 2002 Elsevier Science B.V. All rights reserved.

Keywords: Electron attachment; C_2F_5I; Clusters; Dissociative electron attachment

1. Introduction

Halogenated hydrocarbons are effective scavengers of low energy electrons. Although these compounds usually possess a positive adiabatic electron affinity, electron attachment to single gas phase molecules generates halogenide ions X^- via dissociative electron attachment (DA) [1,2], viz.

$$e^-(\varepsilon) + M \rightarrow M^{-\#} \rightarrow R + X^- \qquad (1)$$

DA is a two-step process where initially a transient negative ion $M^{-\#}$ (TNI) is formed at a particular resonance energy (ε) which in the second step decomposes into a neutral radical and a negative ion. Only at higher pressures or when the TNI is coupled to some dissipative environment (like in a van der Waals cluster), collisional stabilization can become sufficiently effective to yield thermodynamically stable parent anions M^- [3,4].

In this contribution we study electron attachment to single C_2F_5I molecules in an effusive molecular beam and to C_2F_5I clusters in a supersonic beam formed by adiabatic expansion of C_2F_5I seeded in Ar or He. While the corresponding methane compound, CF_3I, has extensively been studied in beam and swarm experiments (see, e.g., the review by Christophorou and Olthoff [5]), for the present molecule we only find

---

[*] Corresponding author. E-mail: iln@chemie.fu-berlin.de
[1] Permanent address: Department of Plasmaphysics, Comenius University Bratislava, 84248 Bratislava, Slovak Republic.

1387-3806/02/$ – see front matter © 2002 Elsevier Science B.V. All rights reserved.
PII S1387-3806(02)00668-1

data on the electron attachment rate obtained from a swarm experiment [6].

CF_3I captures electrons within a narrow resonance close to 0 eV exclusively decomposing into $I^- + CF_3$ (selective bond cleavage), since the other DA channel into $F^- + CF_2I$ is energetically inaccessible at that electron energy. An additional resonance located at 3.8 eV decomposes into the ion fragments F^-, FI^- and $CF_3{}^-$ [7]. The recommended cross section for the attachment of thermal electrons to CF_3I is $\approx 5 \times 10^{-14}\,\mathrm{cm}^2$ based on the analysis of swarm and beam experiments [5]. In C_2F_5I the pulse radiolysis swarm method [6] yields a thermal attachment rate coefficient of $2 \times 10^{-8}\,\mathrm{cm}^3\,\mathrm{s}^{-1}$. Rate coefficient k_T and cross section $\sigma(\upsilon)$ are related by

$$k_T = \int_0^\infty f_T(\upsilon)\upsilon\sigma(\upsilon)\,\mathrm{d}\upsilon = \langle\upsilon\rangle\langle\sigma\rangle$$

where $f_T(\upsilon)$ is the normalized velocity distribution of the electrons at temperature T. For a standard Maxwell–Boltzmann velocity distribution the mean velocity is given by $\langle\upsilon\rangle = (8kT/\pi m)^{1/2}$ corresponding to $1.08 \times 10^7\,\mathrm{cm\,s}^{-1}$ at 300 K. The above rate coefficient hence corresponds to an average cross section of $2 \times 10^{-15}\,\mathrm{cm}^2$ indicating that C_2F_5I is a considerably weaker electron scavenger.

2. Experimental

The experiments are performed in a crossed electron beam/molecular beam arrangement as described previously [7]. The electron beam is generated by a *trochoidal electron monochromator* [8] operating with a homogeneous magnetic field which aligns the electrons and prevents spreading of the beam towards low energies. Clusters are produced by adiabatic expansion of C_2F_5I seeded in Ar or He through a 80 μm nozzle at room temperature. After passing a skimmer (separating the expansion chamber from the main chamber), the molecular beam containing a *size distribution* of clusters is crossed with the electron beam. Alternatively, molecules can be introduced via a capillary which is directly fitted to the reaction chamber (effusive gas inlet). Negative ions formed by crossing the electron beam with either the effusive molecular beam or the supersonic molecular beam are extracted from the reaction chamber by a small electric field ($<1\,\mathrm{V\,cm}^{-1}$), analyzed by a commercial quadrupole mass spectrometer and detected by single pulse counting electronics. For the present experiments the resolution of the electron beam was about 0.25 eV (FWHM) at a current of 50 nA. The electron energy scale is calibrated by means of the “0 eV” resonance in SF_6. For the *effusive beam* experiments the pressure was in the 10^{-6} mbar region as recorded by an ionization gauge at one of the flanges. In the collision region the pressure is by 2–3 orders of magnitude higher. In the *supersonic beam* experiments the background pressure was in the 10^{-5} mbar range at stagnation pressures up to several bars.

3. Results and discussion

3.1. Gas phase molecules

Fig. 1 presents the ion yield curves of the two fragments observed in electron attachment to single C_2F_5I molecules. As expected, the prominent fragment is I^- appearing from a narrow resonance close to 0 eV. An additional resonant I^- feature is located at 2.3 eV. The weaker fragment, F^-, is formed within a structured contribution consisting of three overlapping resonances with peak maxima at ≈2.3, 4 and 5.4 eV as indicated by the dotted curves in Fig. 1. A weak and narrow F^- signal is also seen near 0 eV which cannot be the result of a primary DA process. It should be noted that neither $CF_3{}^-$ nor $C_2F_5{}^-$ (which, e.g., appear from DA to C_2F_6 [9,10] could be observed within the detection limit of the present experiment.

The thermodynamic threshold (ΔH_0) for the formation of the two observed ionic fragments X^- is given by $\Delta H_0 = D(\mathrm{C{-}X}) - \mathrm{EA}(\mathrm{X})$ with D the bond dissociation energy and EA(X) the electron affinity of the corresponding halogen atom. While the $I{-}C_2F_5$ bond dissociation energy is known (2.27 eV [11]) there is no number available in the literature for the $F{-}C_2F_4I$

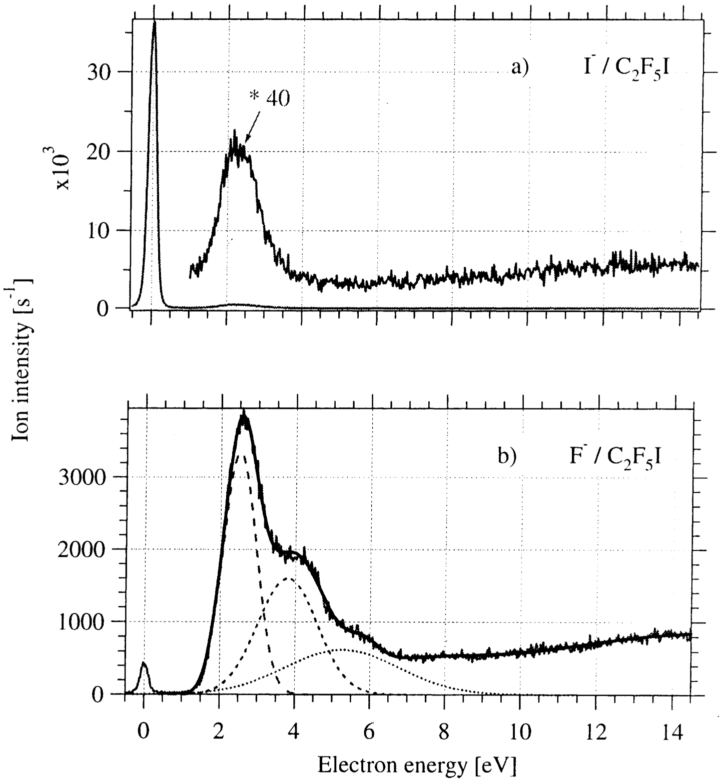

Fig. 1. Formation of I^- and F^- from single C_2F_5I molecules (effusive beam) at a pressure of 2×10^{-6} mbar at the ionization gauge. Ion count rates in absolute numbers. The dotted curves represent three overlapping Gaussian resonances summing up to the measured curve.

dissociation energy. If we assume the same value as estimated in iodomethane ($D(\text{F–CF}_2\text{I}) = 4.9\,\text{eV}$ [12]) and use $\text{EA(F)} = 3.40\,\text{eV}$ and $\text{EA(I)} = 3.06\,\text{eV}$ [11] (we give here only two decimal digits of the very well known atomic electron affinities), we arrive at the following energetic limits:

$$e^- + C_2F_5I \rightarrow C_2F_5 + I^-, \quad \Delta H_0 = -0.79\,\text{eV} \tag{2a}$$

$$e^- + C_2F_5I \rightarrow C_2F_4I + F^-, \quad \Delta H_0 = 1.5\,\text{eV} \tag{2b}$$

Formation of F^- near 0 eV is thus not possible via a primary DA reaction. It should be noted that in endothermic DA reactions peaks can in fact appear near 0 eV due to processes involving vibrationally excited states [13]. Due to the considerable endothermicity of reaction (2b), however, this is an extremely unlikely explanation and the origin of the small F^- signal near 0 eV remains unclear. A possible explanation is thermal decomposition of the target molecule at the hot filament forming F_2 which can reach the reaction volume and undergo effective DA yielding F^- with a peak close to 0 eV [14]. This explanation is also corroborated by the present cluster results (Fig. 6).

When comparing C_2F_5I and CF_3I it is obvious that both compounds show an intense 0 eV resonance exclusively generating I^-, with the cross section being one order of magnitude lower in C_2F_5I. It is very likely that the low energy process in C_2F_5I (as in CF_3I) involves a one particle shape resonance with pronounced σ^*(C–I) character. In CF_3I this resulted in direct electronic dissociation along the repulsive C–I potential energy surface with 87% of the available excess energy appearing as translational energy of the two products $CF_3 + I^-$ [12]. An impulsive dissociation into $I^- + C_2F_5$ is also observed in the present case, however, with less translational energy due to effective rotational excitation of the C_2F_5 radical [15].

In CF_3I a second resonance was located at 3.8 eV decomposing into $CF_3{}^-$ but *not* into I^-. This second resonance was interpreted as a core excited (two particle) state due to excitation of an electron from the iodine atom to the σ^*(C–I) MO, and hence a state with two electrons in the antibonding σ^* MO. This explains the high translational energy of the $CF_3{}^-$ fragment and also the absence of I^- since localization of *both* σ^* electrons onto the dissociating (initially positively charged) iodine is unlikely. In the present compound the situation is considerably different since the second feature (as observed on the F^- channel) is composed of three overlapping resonances. Out of these only from the lowest one (located near 2.5 eV) both fragments, F^- and I^- appear (Fig. 1). Since the energy of the first electronic excitation is very similar in CF_3I and C_2F_5I [16] we interpret the feature near 4 eV as (open or closed channel) core excited resonance associated with the first electronic state. The lower feature at 2.6 eV is then attributed to a single particle resonance while that at 5.4 eV is correlated to some higher electronic state of C_2F_5I.

3.2. Clusters

3.2.1. Negative ion mass spectra

Fig. 2 shows negative ion mass spectra from the C_2F_5I cluster beam recorded at an electron energy (a) close to 0 eV and (b) at 2.5 eV. The beam was generated by adiabatic expansion of C_2F_5I seeded at high excess of Ar (1:100). At that mixing ratio we detect a series of negatively charged complexes containing Ar, namely $Ar_n{\cdot}I^-$ ($n = 1$–16) and, most notably, ternary cluster ions of the form $Ar_n{\cdot}M{\cdot}I^-$ ($M = C_2F_5I$, $n =$ 1–10). In this notation we have assumed that in complexes containing both the undissociated molecule (M) and the fragment X (X = I, F) the additional charge is localized on the halogen atom due its considerably higher electron affinity. Although the electron affinity of C_2F_5I is not directly known, but it may be close to that of CF_3I where the literature values scatter between 1.4 and 2.2 eV [12]. Along the series $Ar_n{\cdot}I^-$ in Fig. 2a, the obvious intensity discontinuity at $n = 3$ arises from an additional contribution of M^- (246 amu) to $Ar_3{\cdot}I^-$ (247 amu). These two compounds cannot be resolved by the presently used mass spectrometer. The subsequent series of mass peaks $Ar_n{\cdot}I^-$ ($n > 3$) may hence also contain $Ar_{n-2}{\cdot}M^-$ each of them differing by one atomic mass unit. Near 370 amu, the partly resolved double peak arises from $Ar_6{\cdot}I^-$ (367 amu) and $Ar_3{\cdot}M^-$ (366 amu) (unresolved lower mass peak) and $M{\cdot}I^-$ (373 amu, upper mass peak). The following series of double peaks is then due to the successive addition of an Ar unit. The relatively prominent peak near 610 amu, finally, is composed of $Ar_{12}{\cdot}I^-$ (607 amu), $Ar_6{\cdot}M{\cdot}I^-$ (613 amu) and $M_2{\cdot}I^-$ (619 amu). The two peaks on the lower mass scale arise from F^- (19 amu) and Cl^- (35/37 amu), the latter due to some impurity. A small contribution from the calibration gas ($SF_6{}^-$) is also seen at 146 amu.

The mass spectrum recorded at 2.5 eV differs in the way that F^- is now more pronounced leading to the additional observation of $M{\cdot}F^-$ (265 amu) and $M_2{\cdot}F^-$ (511 amu). The series $Ar_n{\cdot}I^-$ is comparatively weak (in accordance with the ion yield curves, see below) so that $Ar_6{\cdot}I^-$ (367 amu) is only seen as a weak shoulder of the dominant $M{\cdot}I^-$ peak (373 amu). There is no indication of complexes of the form $Ar_n{\cdot}F^-$. Such complexes (up to $n = 4$) were recently observed in electron attachment to a beam formed in an NF_3/Ar expansion [17].

The appearance of anionic complexes containing Ar units is strongly suppressed when the amount of Ar is reduced in the expanding mixture as illustrated in Fig 3a. This mass spectrum was obtained from a 1:30 mixture at a stagnation pressure of 1 bar and recorded at 0 eV. In this case the complexes $Ar_n{\cdot}I^-$ are only observed up to $n = 5$. The parent negative ion is comparatively weak (246 amu coinciding with $Ar_3{\cdot}I^-$) while the solvated ions $M_n{\cdot}I^-$ are the only products present above 330 amu. Fig. 3b shows a mass spectrum from an expansion using He as seed gas. As expected, no clusters containing the seed gas atoms are observed

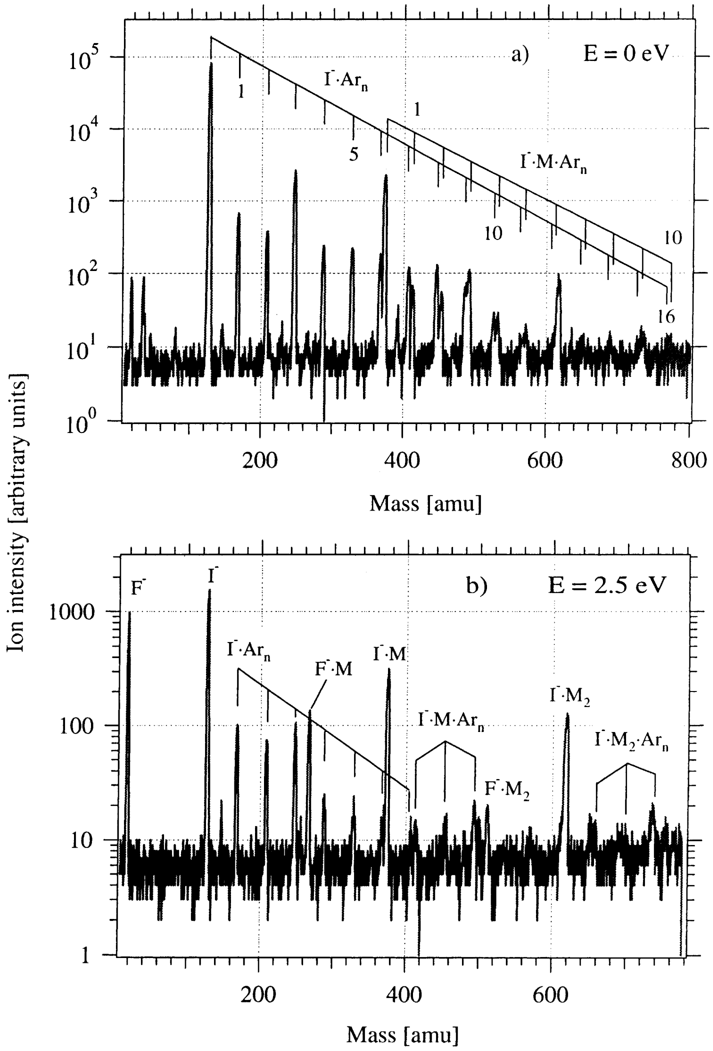

Fig. 2. Negative ion mass spectra obtained from an expansion of C_2F_5I seeded in Ar (1:100), (a) at an electron energy close to 0 eV and a stagnation pressure of 2 bar, (b) at an electron energy of 2.5 eV and a stagnation pressure of 2.5 bar. The discontinuity in the homologous series $Ar_n\cdot I^-$ at $n = 3$ (247 amu) arises from an unresolved contribution of M^- (246 amu, $M = C_2F_5I$).

and the overall formation of molecular clusters is obviously much less effective. The peak at 247 amu, on the other hand, can now unambiguously be identified as the parent negative ion.

3.2.2. Ion yield curves

Fig. 4 presents the ion yield curves for the products I^-, $Ar\cdot I^-$ and $M\cdot I^-$ obtained from electron attachment to the cluster beam at a mixing ratio of 1:100 and a stagnation pressure of 1 bar. It should be noted that the fragment I^- can either be a product of DA to a monomer (from scattered background molecules or monomers traveling in the molecular beam) or the result of electron capture to a cluster. The complexes $Ar\cdot I^-$ and $M\cdot I^-$, on the other hand, are necessarily products of an electron attachment reaction to a cluster. In the range 0–3 eV the $Ar\cdot I^-$ ion yield curve resembles that of I^- observed from isolated molecules,

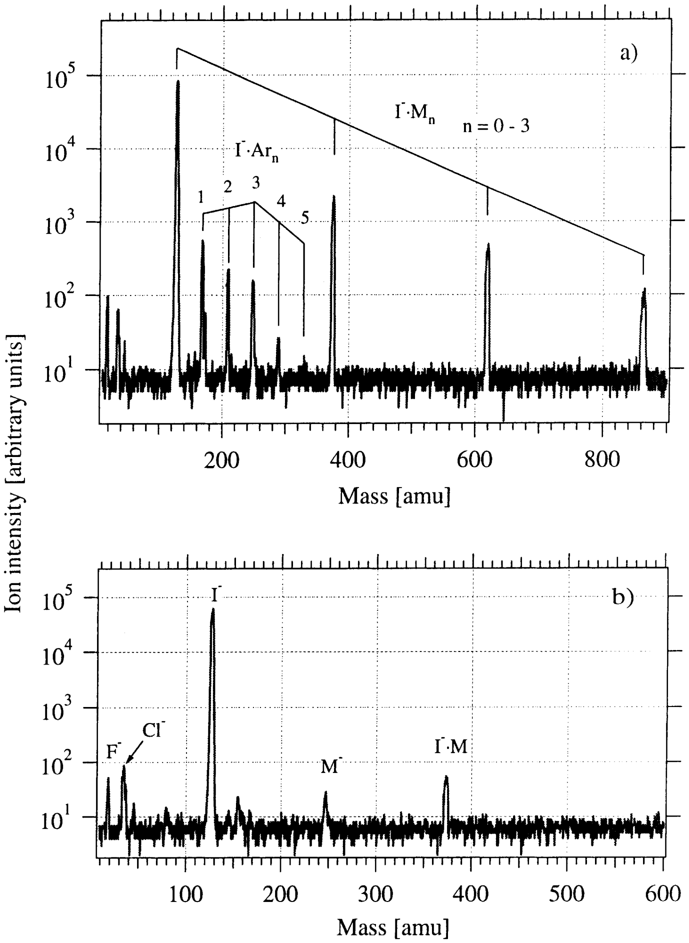

Fig. 3. Negative ion mass spectra obtained at an electron energy close to 0 eV from an expansion of C_2F_5I seeded in (a) Ar (1:30), stagnation pressure 1 bar, and (b) He (1:100), stagnation pressure 2.5 bar. Due to the absence of $Ar_n{\cdot}I^-$ complexes in (b) the undissociated anion (M^-) is unambigously identified at 246 amu.

however, with an additional feature near 6 eV. On the channel $M{\cdot}I^-$ several higher energy structures become appreciably intense and on the $M_2{\cdot}I^-$ channel (not shown here), the ion intensity in the range 2–6 eV is even on the same scale to that of the resonance at 0 eV.

It is clear that any solvated fragment ion (like $M{\cdot}I^-$) must originate from an initial intracluster DA process. In the isolated molecule, DA is essentially restricted to the 0 eV resonance with a comparatively small additional contribution around 2.3 eV (Fig. 1). On the solvated ion channel, the signal at energies *beyond* 0 eV is comparatively more intense as can be seen from the multiplication factors. This signal is likely to originate from inelastic scattering processes in the target cluster, i.e. inelastic scattering of the incoming fast electron and transfer of the slowed down electron to a second C_2F_5I molecule which undergoes DA ultimately forming a solvated ion ($Ar_n{\cdot}I^-$ or $M_n{\cdot}I^-$) by evaporating the neutral units. The inelastic scattering processes can involve electronically excited states or resonances of C_2F_5I. Such *autoscavenging* processes are common features in clusters containing strong scavengers of 0 eV electrons [7,18,19] These features

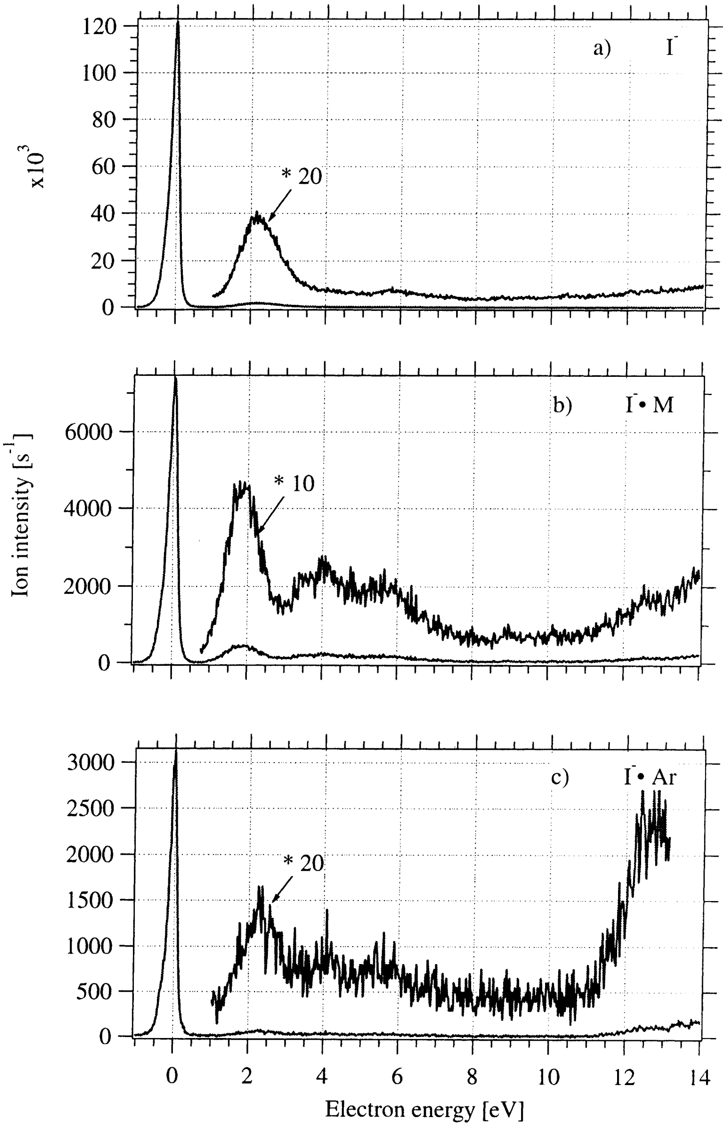

Fig. 4. Ion yields of some product ions recorded from the beam generated by an expansion of C_2F_5I seeded in Ar (1:100) at a stagnation pressure of 1 bar. The atomic fragment I^- can also arise from DA to monomers. The continuously rising signal above ≈11.5 eV is due to Ar metastables from the seed gas which are excited in electron impact.

hence represent *threshold excitation spectra* of the molecule in a cluster. The features near 4 and 5.4 eV are attributed to core excited resonances related to electronically excited states of the neutral molecule, and that near 2 eV to a one particle shape resonance. For the shape resonance, autodetachment creating vibrational excitation in the neutral molecule represents the underlying inelastic scattering mechanism.

It is interesting to note that formation of the undissociated monomer ion (M^-) is considerably weaker than that of the solvated fragment ion ($I^-{\cdot}M$), a fact which is independent of the stagnation pressure. The corresponding reactions (not considering the presence of Ar units) can be expressed as

$$e^- + M_n \rightarrow M^{-\#} \cdot M_{n-1} \rightarrow I^- \cdot M + R + (n-2)M \tag{3a}$$

$$e^- + M_n \rightarrow M^{-\#} \cdot M_{n-1} \rightarrow M^- + (n-1)M \tag{3b}$$

with $R = C_2F_5$. The energetics for both processes are presumably close to each other since the exothermicity of the DA channel (3a) plus the binding energy of the complex $I^- \cdot M$ may roughly sum up to the electron affinity of M. There is hence no obvious energetic argument why (3a) should be favored over (3b). This may rather be a mirror of the preferential pathway in the short time domain (femtoseconds to picoseconds) after electron localization. Once the transitory negative ion $C_2F_5I^{-\#}$ is formed within the cluster it may in the first step rather separate into $C_2F_5 + I^-$ (pathway ① in Fig. 5) than be trapped in a state below the dissociation limit (pathway ②). The impulsive dissociation hence prevails over the caging effect of the surrounding particles.

In all the cluster spectra there is some continuously rising signal at energies above ≈11.5 eV which is independent of mass separation or ion extraction condition. We attribute this signal to excitation of metastable Argon atoms ($^3P_{0,2}$) from the carrier gas which accidentally reach the detector. The excitation energy for the low lying state ($^3P_2$) is 11.55 eV [20] and thus sufficient to emit an electron from the first dynode of the electron multiplier. This signal has some peak like structure near 12.5 eV which we have observed before when Ar was used as carrier gas. The origin of this structure is not yet clear; it cannot arise from the different spin orbit states as the fine structure splitting is only 0.1 eV.

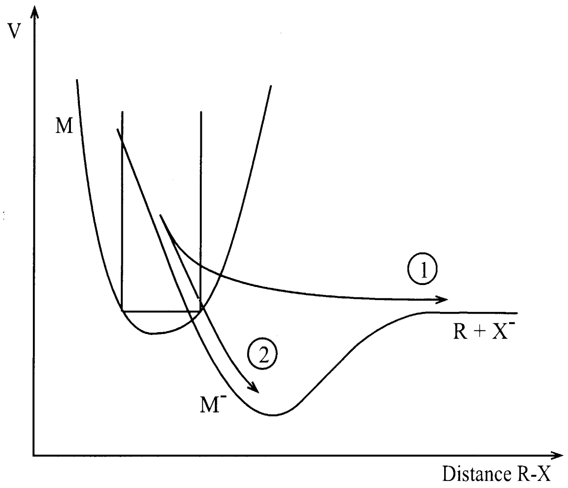

Fig. 5. Schematic potential curves illustrating the evolution of the transient ion $C_2F_5I^{-\#}$ generated in a cluster. Pathway ① is intracluster DA leading to solvated ions $M_n \cdot I^-$ and ② collisional stabilization forming the monomer anion (evaporative attachment).

Fig. 6 presents the F^- and $M \cdot F^-$ channel obtained from electron attachment to the cluster beam (mixing ratio 1:100, stagnation pressure 1 bar). While the F^- yield virtually coincides with that from the isolated molecule (as it partly also results from monomers), the $M \cdot F^-$ channel is restricted to a single resonance peaking at 2 eV. Since F^- cannot be formed via the strong 0 eV resonance, autoscavenging can be excluded and $M \cdot F^-$ originates from an initial DA reaction in the cluster. We have then obviously a situation where the core excited states are strongly quenched by the environment, a situation which has been observed before in CF_3Cl [7]. $M \cdot F^-$ is pedominantly formed from the shape resonance near 2 eV, with a remarkable shift of the resonance position with respect to the F^- channel. This downshift is also obvious on the solvated ion $M \cdot I^-$ (Fig. 4). It must be noted that the resonance position observed on a product ion mirrors both the energy of the initial Franck–Condon transition, but also the energy dependent probability to form the particular ion under observation. When proceeding from isolated molecules to clusters, resonances observed on DA channels can hence be shifted to lower or to higher energies. In the latter case, the solvation shift in the initial transition is overbalanced by the energy dependent decomposition probability.

It is finally interesting to note that the $M \cdot F^-$ signal arising from intracluster DA does not show any signal at 0 eV. This supports the picture of thermal decomposition of C_2F_5I at the hot filament creating F_2 which, once reaching the reaction volume, can produce F^- at 0 eV.

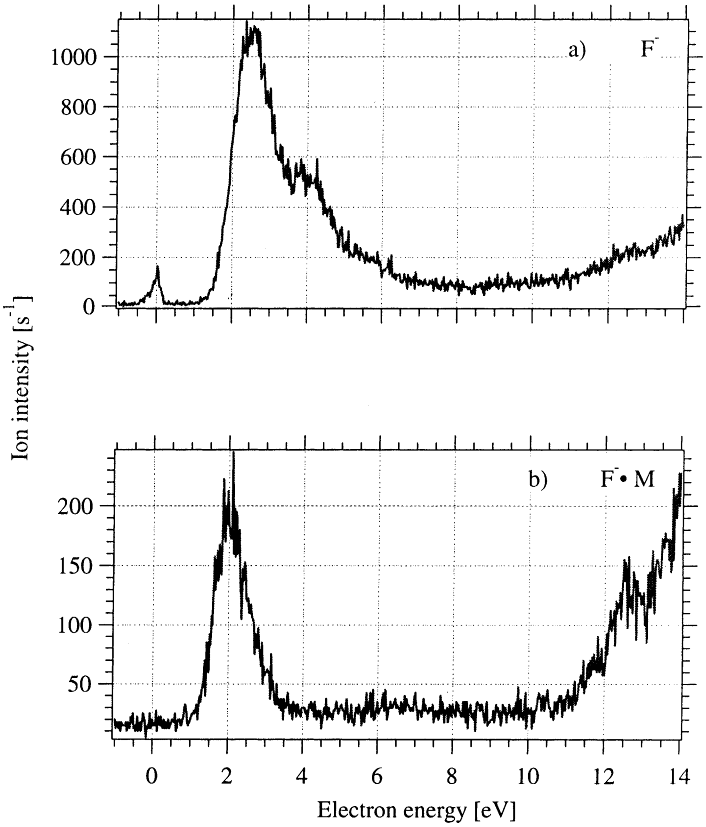

Fig. 6. Ion yields of F$^-$ and M·F$^-$ recorded from the supersonic beam at the conditions of the spectra in Fig. 4. The resonance maximum for the solvated ion is shifted to lower energy and the peak at 0 eV is no longer present (see the text).

Acknowledgements

This work has been supported by the Volkswagen Siftung (I/73593), the Deutsche Forschungsgemeinschaft (Il 16/15-1) and the Freie Universität Berlin.

References

[1] L.G. Christophorou (Ed.), Electron–Molecule Interactions and their Applications, Vol. I, Academic Press, Orlando, FL, 1984.

[2] E. Illenberger, J. Momigny, Gaseous Molecular Ions. An Introduction to Elementary Processes Induced by Ionization, Steinkopff Verlag, Darmstadt/Springer, New York, 1992.

[3] T.D. Märk, Int. J. Mass Spectrom. Ion Process. 107 (1991) 143.

[4] E. Illenberger, Electron capture processes by free and bound molecules, in: C.-Y. Ng (Ed.), Advanced Series in Physical Chemistry, Vol. 10B, Photoionization and Photodetachment, Part II, World Scientific, Singapore, 2000.

[5] L.G. Christophorou, J.K. Olthoff, J. Phys. Chem. Ref. Data 29 (2000) 553.

[6] T. Sunagawa, H. Shimamori, in: Y. Hatano, H. Tanaka, N. Kouchi (Ed.), Proceedings of the International Symposium on Electron–Molecule Collisions and Swarms, Tokyo, 18–20 July 1999, p. 181.

[7] O. Ingólfsson, F. Weik, E. Illenberger, Int. J. Mass Spectrom. Ion Process. 155 (1995) 1 (Review).

[8] A. Stamatovic, G.J. Schulz, Rev. Sci. Instrum. 41 (1970) 423.

[9] R. Hashemi, Diplome Thesis, Freie Universität Berlin, 1990.

[10] F. Weik, E. Illenberger, J. Chem. Phys. 103 (1995) 1406.

[11] D.R. Lide (Ed.), Handbook of Chemistry and Physics, 78th Edition, CRC Press, Boca Raton, 1997.

[12] T. Oster, O. Ingólfsson, M. Meinke, T. Jaffke, E. Illenberger, J. Chem. Phys. 99 (1993) 5141.

[13] I. Hahndorf, E. Illenberger, Int. J. Mass Spectrom. Ion Process. 167/168 (1997) 87.
[14] W.C. Tam, S.F. Wong, J. Chem. Phys. 68 (1978) 5626.
[15] J. Langer, S. Matejcik, E. Illenberger, Phys. Chem. Chem. Phys., submitted for publication.
[16] M.B. Robin, Higher Excited States of Polyatomic Molecules, VoI. I (1974) and Vol. III (1985), Academic Press, New York.
[17] J. Langer, S. Matejcik, E. Illenberger, Phys. Chem. Chem. Phys. 2 (2000) 1001.
[18] E. Illenberger, Chem. Rev. 92 (1992) 1589.
[19] M. Foltin, V. Grill, T.D. Märk, Chem. Phys. Lett. 188 (1992) 427.
[20] C.E. Moore, Atomic Energy Levels, National Bureau of Standards, NSRDS–NBS 35, Washington, 1971.